Branislav Đorđević[1], Aleksandar Sedmak[2], Blagoj Petrovski[1], Simon Sedmak[1], Zoran Radaković[2]

LOAD AND DEFORMATION EFFECTS ON BRITTLE FRACTURE OF FERRITIC STEEL 20MnMoNi 55 IN TEMPERATURE TRANSITION REGION

UTICAJI OPTEREĆENJA I DEFORMACIJE NA KRTI LOM CEPANJEM FERITNOG ČELIKA 20MnMoNi 55 U PODRUČJU PRELAZNE TEMPERATURE

Originalni naučni rad / Original scientific paper
UDK /UDC:

Rad primljen / Paper received: 30.09.2020

Adresa autora / Author's address:
[1)] University of Belgrade, Innovation Centre of the Faculty of Mech. Eng., Serbia email: b.djordjevic88@gmail.com
[2)] University of Belgrade, Faculty of Mech. Engng., Serbia

Keywords
- transition region
- 20MnMoNi 55 ferritic steel
- brittle fracture
- displacement rate

Ključne reči
- područje prelazne temperature
- feritni čelik 20MnMoNi 55
- krti lom
- brzina ispitivanja

Abstract

It is known that the load level, the way deformation is applied and the level of plastic strain, all can ‘aid’ or ‘hinder’ the occurrence of brittle fracture, but the question is - to what extent? These influential factors are analysed by testing of C(T)50 specimens made of ferritic steel 20MnMoNi 55 at two temperatures within the transition temperature range. The effect of displacement rates is analysed by testing C(T) specimens at -60 °C, while the effect of plastic strain is analysed by introducing an initial fatigue crack with low and high stress intensity factor threshold values of ΔK, by testing the C(T) specimens at -90 °C, in accordance with ASTM 1820 standard. The analysis of these influences involves interpretation of test results for parameters J_c, CMOD, and r_c. Conclusions based on this analysis can be used in further studies which involve understanding of ductile to brittle transition region, as well as the general fracture behaviour of ferritic steels.

Izvod

Poznato je da nivo opterećenja, način zadavanja deformacije, ali i nivo plastične deformacije 'pomažu' ili 'odmažu' pojavu krtog loma, ali ostaje pitanje - u kojoj meri? Ovi uticaju analizirani su ispitivanjem C(T)50 epruveta feritnog čelika 20MnMoNi 55 na dve ispitne temperature u prelaznom temperaturskom režimu. Uticaj brzine ispitivanja, tačnije, nivo zadate deformacije je analiziran ispitivanjem C(T) epruveta na -60 °C. Uticaj plastične deformacije je analiziran unošenjem inicijalne zamorne prsline sa niskom i visokom vrednošću opsega ΔK na C(T) epruvetama, a ispitivanja su ovom slučaju urađena na temperaturi -90 °C. Ispitivanja su rađena prema odgovarajućem standardu ASTM 1820. U analizi ovih uticaja tumačeni su rezultati parametara J_c, CMOD i parametra r_c, koji je objašnjen. Zaključci u radu mogu poslužiti za dalji tok studija koje se tiču razumevanja prelaza iz žilavog u krti lom, i generalno krtog loma feritnih čelika.

INTRODUCTION

It is well known that brittle fracture occurs at very low or non-existent plastic strain in a material, especially in a metallic material. It often occurs at an unpredictable stress level, during sudden unstable crack growth. Simply put, brittle fracture is always unwanted in metallic structures. Ever since the Liberty ships’ failure studies, it is known that ferritic steels are sensitive to temperatures that decrease brittle fracture, making it more likely to occur. Brittle fracture is characterised by a very low level of its initiation energy and by the absence of plastic strain. One of the basic differences between brittle and ductile fracture is that in the case of brittle fracture, crack growth is not affected by plastic strain, as opposed to ductile fracture. From an engineering point of view, brittle fracture involves minimal plastic strain of fractured surfaces, conditionally referred to as brittle fracture /1-5/. With the decrease of working temperature, most materials change their mechanism of fracture to brittle. This process is very complex and is known as the transition temperature region. Some of the general macroscopic characteristics of brittle fracture, visible on tested specimens, or a real structure, include:

- fracture is preceded by negligible plastic strain,
- crack growth rate is fast, fracture is sometimes accompanied with a quite noise,
- specimen fracture surface is flat and perpendicular to the load direction,
- fracture surface structure is crystal-like, with a large number of planes with light reflections,
- during tensile tests, there is no necking of the specimen prior to fracture (or it is too small to observe),
- characteristic arrow-shaped patterns can be observed on the fracture surface of the tested specimens of structures.

In general, it is not possible to draw a distinction and a clear line between brittle and ductile fracture, since every fracture possesses a certain, sometimes negligible, but still present level of plastic strain. The fact remains that metallic materials in real conditions do not exhibit pure brittle fracture behaviour, even at lower temperatures, and that this scenario should thus be referred to as quasi-brittle failure /6-8/. These quasi-brittle failures of ferritic materials are often called brittle in practice, since ideal Griffith curves for brittle failure of metallic materials do not exist.

DUCTILE TO BRITTLE FRACTURE TRANSITION

The material structure is such that brittle fracture is dependent on load levels and exploitation conditions. For most structural materials of ferritic crystal structure, brittle fracture is more likely to occur under conditions such as lower temperatures, load (e.g. increase in force magnitude). The same material having different applications in terms of exploitation conditions can behave either as plastic or brittle, depending on the conditions previously mentioned. A topic of numerous studies over the years, including /9-15/, involves the extent of working condition necessary to change the nature of fracture, from ductile to brittle. In general, this change depends on material properties, in this case for steel 20MnMoNi 55 /16, 17/, i.e. it depends on its general sensitivity to temperature changes. Conditions under which materials, particularly ferritic steels, change their fracture mechanism from ductile to brittle depend on:

(a) shape and dimensions of the structural element in exploitation or in the tested specimen;
(b) load and displacement rate of the workpiece or tested specimen;
(c) work or test temperatures.

As it is well known, stress values and distribution at certain load levels depend on stress concentration and plastic zone size. Plane stress and strain state contribute to plastic and brittle fracture, respectively. Under plane stress state, fracture is plastic (ductile), wherein under plane strain conditions, it is brittle. One of the ways of achieving plane strain state in specimens is to take into account specimen thickness /17-19/. Specimens can have different shapes (C(T), Charpy, disk-shaped specimens etc.), depending on standards used for testing, such as in /20, 21/. The greater the thickness, the more prominent the plane strain state which contributes to brittle fracture, as reflected on the relevant measured fracture parameters in each test method.

Change of test rate in certain cases can affect the change of material mechanical properties, or the selection of the relevant fracture mechanics parameter. In standard tests, performed for the purpose of determining basic mechanical properties, as well as fracture mechanics parameters, there are two distinctive techniques for defining the loads during the test, i.e. the deformation process rate. The displacement rate for a given specimen can be defined by:

– changing the load over time (load control). In this case the force increment is constant, and if the strain during the deformation process is small, the following relation can be written for determining the displacement rate:

$$V_S = \frac{d\sigma}{dt}\,. \qquad (1)$$

– changing the deformation over time (displacement rate control). In this case, assuming the elongation is small compared to the initial value, the rate of the grips used to define the change in load can be written as:

$$V_k = \frac{d\varepsilon}{dt}\,. \qquad (2)$$

Depending on the testing rate, metals can be divided into those not sensitive to it, and those whose mechanical properties change with this rate. This can be even more noticeable in fracture mechanics parameters. If the test temperature is added as a factor to these conditions, problems will occur involving the interpretation of the relevant parameter value scatter, especially prominent in the transition temperature region. Figure 1 shows the choice of a relevant fracture mechanics parameter depending on test temperature. The general rule is that an increase in deformation leads to an increase in plastic zone size, resulting in material hardening that delays the fracture, thus completely avoiding brittle failure, but this is not necessarily the case. In the following chapters of this study, the combined influence of test rate and temperature on brittle fracture are shown, using the corresponding parameters.

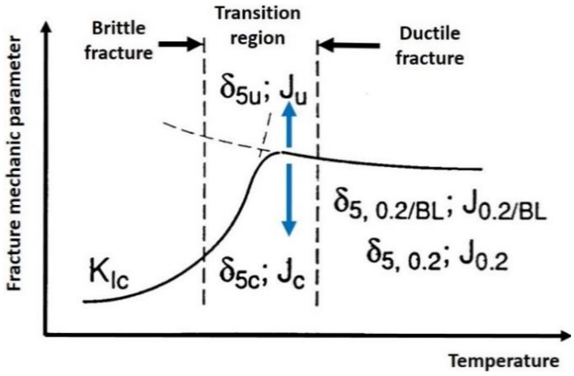

Figure 1. Influence of temperature on the selection of relevant fracture mechanics parameter, /22/.

EXPERIMENTS

Steel 20MnMoNi55 and its mechanical properties

C(T)50 specimens in this study are made of ferritic reactor steel 20MnMoNi 55 (according to DIN) of chemical contents and mechanical properties at room temperature given in Tables 1 and 2, respectively. Specimens are cut out of a plate. The steel is used for pressure vessels and power plant reactors and is generally meant for extreme conditions, and as such is studied in /16, 17, 23, 24/. However, it is necessary to select the main studies concerning this steel, which include Heerens /16/, who identified the mechanisms and types of cleavage fracture. This study partially relies on his work. The main focus of other studies involves the properties and the behaviour of this steel in the transition temperature region, for the purpose of structural integrity assessment of pressure vessels, reactors, storage tanks etc., and for determining the capabilities and limitations of its applications. This steel is similar to American steel type A533B.

Preparation of C(T) specimens

This study involves the testing of C(T)50 specimens at temperatures -60 °C and -90 °C. Two different net values of thicknesses are used, 16 mm C(T)50 specimens for testing at -60 °C, and 20 mm specimens for testing at -90 °C.

Table 1. 20MnMoNi55 steel chemical composition in wt. %, /16/.

C	Si	Mn	Cr	V	Cu	Al
0.19	0.2	1.29	0.12	0.02	0.11	0.015
Ni	Mo	Co	As	Sb	Ti	
0.8	0.53	0.014	0.030	0.03	0.05	

Table 2. Mechanical properties of steel at room temperature.

Yield strength σ_Y (MPa)	Tensile strength σ_u (MPa)	Elongation (%)
450	610	/

Precracking is performed on all specimens in accordance with standards /21, 25/. For the purpose of the tests defined in the introduction, i.e. the study of plastic strain effect on brittle fracture via SIF threshold ΔK values (K-factor), the precracking is performed with two values of ΔK. A portion of the specimens, specifically those used at -90 °C are precracked with ‘high’ and ‘low’ threshold values. Some of the specimens are precracked with high ΔK = 1230 Nmm$^{-3/2}$ = 38.9 MPa√m, and some of the specimens with low ΔK = 492 Nmm$^{-3/2}$ = 15.6 MPa√m. Precracking of specimens with high ΔK was conducted with 36 500 cycles, while specimens with low ΔK were precracked with 215 000 cycles in the load control condition.

As an illustration of the process, Fig. 2 shows this concept of introducing a fatigue crack, and in this case, the initial crack for a constant value of the K-factor, ΔK. This type of load does not exist in real exploiting conditions, and the load is applied via force. However, this concept is interesting for experiments and is possible to achieve by using computer controlled pulsators, as in the case in this paper, with previously described C(T)50 specimens. It should be noted that the invariability of ΔK during crack growth does not imply that the load $F(P)$ or displacement V_p do not change as well. Quite contrary, in order to achieve needed load levels, the K-factor needs to decrease in a certain way during crack growth, /25/.

Since every fatigue cycle forms a corresponding plastic zone ahead of the crack tip, $r_p^c(\theta)$ in Fig. 2, and the fatigue crack growth leaves an area of plastically deformed material behind its tip. If the plastic zone $r_p^c(\theta)$ is at the same time within the K-dominant singularity zone R_k, the small scale yielding condition is fulfilled, $r_p^c(\theta) < R_k$, thus the K-factor values for the considered fatigue cycle uniquely describe the stress field at the crack tip. The size of the plastic zone only depends on the values of K_{max} and K_{min}, and in this way the influence of the plastic zone and its area on crack growth rate is implicitly taken into account. If K_{max} and K_{min} are varied during fatigue cycles, crack growth for the current cycle can depend on the load level as well.

It can be concluded from the previous text that fatigue crack growth, in this case of an initial fatigue crack, represents a very complex process depending on a large number of variables such as effective stress field intensity at the crack tip, defined by the K-factor, the type and form of load, the environment, mechanical and metallurgical properties of the material, etc. /25, 27, 28/.

Transition temperature experiments

- Influence of displacement rate

Testing of C(T)50 specimens is performed using a commercial test machine of 20 t capacity. The first series of specimens is tested at -60 °C with 20 mm thickness and side grooves of depth equal to 20 % thickness. Testing is performed according to the relevant standard /21/, and with the use of standard /29/. Specimen preparation i.e. fatigue crack initiation is described previously and is done in accordance with a relevant standard. Loading is defined via displacement rate, with 2 displacement rates used in the test. Displacements rates for testing C(T)50 at -60 °C are 0.5 and 0.02 mm/min. Cooling is performed in a liquid nitrogen chamber, where temperature is controlled by ventilation.

Testing is performed at -60 °C. Standard force-displacement curves are then recorded for each specimen and used in order to obtain J_c and crack mouth opening displacement (CMOD) values. CMOD is typically obtained during the plotting of the force vs. displacement diagram, /12, 21/. This parameter is measured on the free surface of the crack,

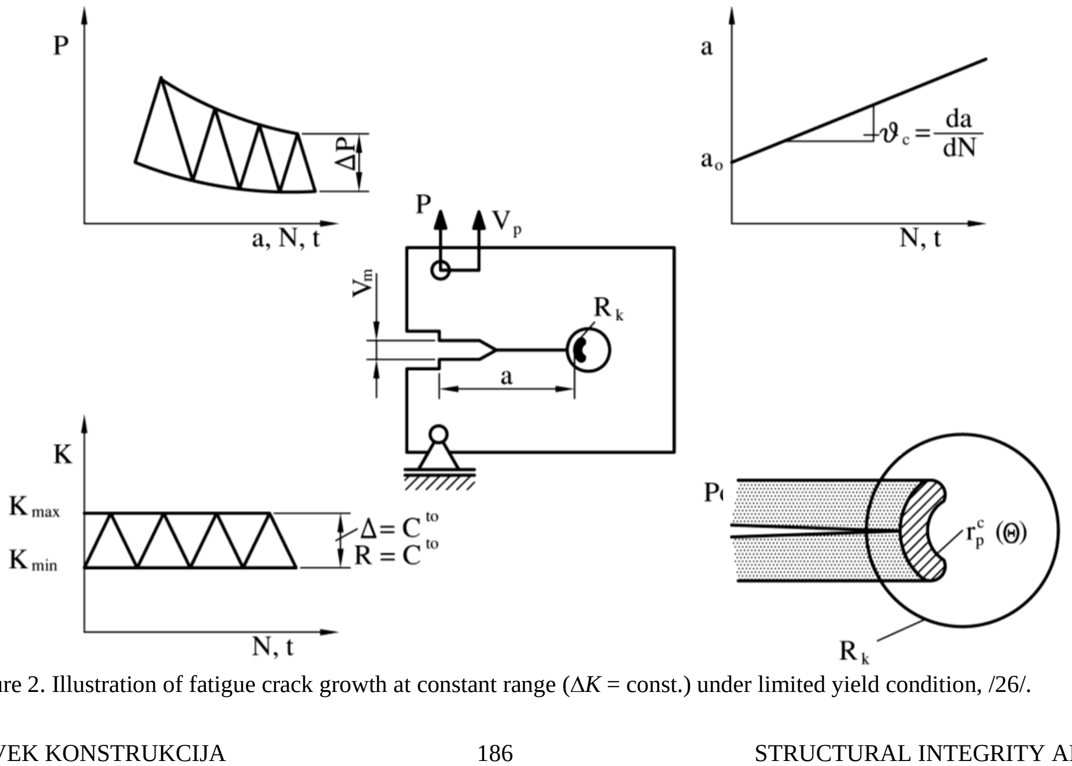

Figure 2. Illustration of fatigue crack growth at constant range (ΔK = const.) under limited yield condition, /26/.

at the location of its maximum opening, and represents the total strain, both elastic and plastic, /6, 12/. The experimental setup is configured such that it ensures the CMOD parameter equals the load-line displacement parameter, as can also be seen in /12, 21/. The setup along with the test specimen is shown in Fig. 3.

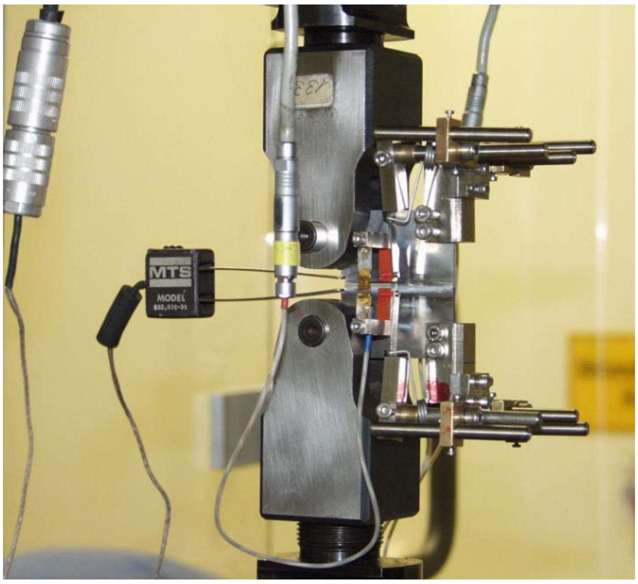

Figure 3. Experimental setup for C(T)50 specimen tests.

The diagram in Fig. 4 shows the comparison of CMOD values of labelled specimens for 0.02 mm/min displacement rate. The CMOD values ranged from 1.049 to 2.315 mm.

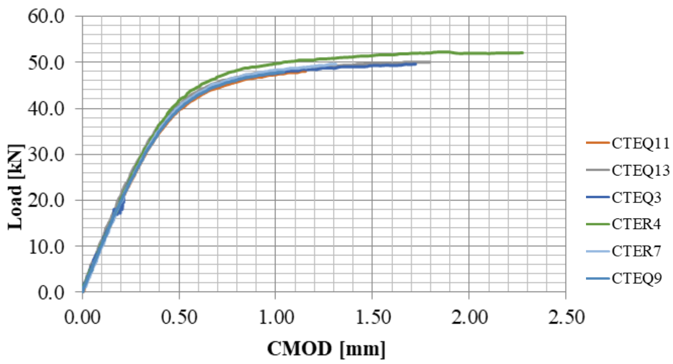

Figure 4. CMOD comparison for C(T)50 specimens at -60 °C and 0.02 mm/min displacement rate.

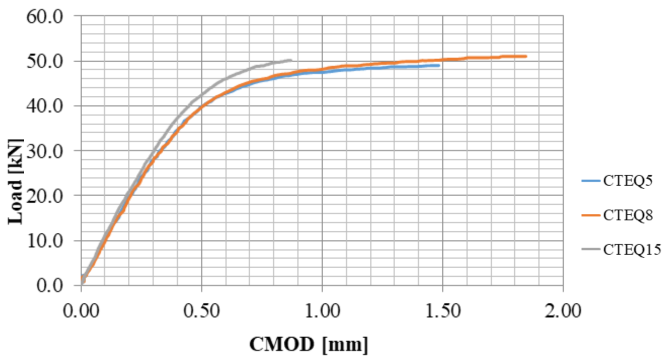

Figure 5. CMOD comparison for C(T)50 specimens at -60 °C and 0.5 mm/min displacement rate.

The diagram in Fig. 5 shows CMOD values for specimens subjected to 0.5 mm/min displacement rate. Specimen labels are also given. CMOD values ranged from 0.896 to 1.852 mm. It can be noticed that these values are lower compared to the ones obtained at slower displacement rate. In both cases and in any other transition temperature range, a scatter of CMOD values is observed, resulting in the scatter of J_c values.

- Influence of precracking on fracture mechanics parameters

In the second series of tests, C(T)50 specimens are tested at -90 °C in the same chamber used in previous experiments. Specimen net thickness is 20 mm, with side groove of depth also equal to 20 % specimen width. Experimental setup and testing is also performed in accordance with standards /21/ and /29/. As previously mentioned, precracking of specimens is performed with two values of Δ*K*. Fatigue crack initiation is performed with a 'high' Δ*K* = 1230 Nmm$^{-3/2}$ = 38.9 MPa√m on a total of 7 specimens, whereas the remaining 9 specimens are precracked with 'low' Δ*K* = 492 Nmm$^{-3/2}$ = 15.6 MPa√m. The aim of this part of research is to determine whether the presence of certain plastic strain ahead of the crack tip will eventually affect the fracture mechanics parameter J_c, thus delaying the cleavage fracture of specimens. An additional parameter is used in this part of the analysis, r_c, represents the distance between the initial crack front and location of cleavage fracture initiation. This parameter is used by Heerens, /16/. Results obtained for J_c and r_c in this study are shown in Table 3.

Table 3. J_c and r_c at -90 °C (without the (*) - precracked with low Δ*K*; with (*) - precracked with high Δ*K*).

Specimen designation	Parameter Jc [N/mm]	Parameter rc [mm]
C(T) Q9	49.4	/
C(T) Q8	49.7	0.15
C(T) Q10	50.6	0.13
C(T) Q7	63.8	0.16
C(T) S2	82.3	0.71
C(T) Q6	121.2	1.00
C(T) Q2	135.2	0.36
C(T) Q3	176	0.36
C(T) Q1	233.6	0.46
C(T) *Q12	84.4	0.31
C(T) *Q13	85.2	0.69
C(T) *Q16	121.3	0.35
C(T) *Q14	129.2	0.42
C(T) *Q11	153.9	/
C(T) *Q15	179.2	0.23
C(T) *S1	270.2	0.69

As can be seen in Table 3 there is noticeable scatter of obtained J_c results for both series of specimens. Slightly higher J_c values are observed in specimens where fatigue crack is initiated with high Δ*K* value. However, the scatter of parameter r_c is larger in specimens precracked with low Δ*K*. Additionally, generally higher values of this parameter are observed at low Δ*K* precracked specimens compared to the high Δ*K* precracked specimens.

CONCLUSIONS

The following conclusions are drawn from the presented test results.

- In the transition temperature region, the scatter of fracture mechanics parameters (under relevant test conditions according to Fig. 1), specifically of CMOD and J_c values, required interpretation using a statistical model.
- Testing of C(T)50 specimens at -60 °C for two displacement rates had shown the influence of this factor on brittle fracture through CMOD values. Higher displacement rate of 0.5 mm/min resulted in lower CMOD values compared to the lower rate of 0.02 mm/min. However, this did not affect the values of J_c. Additionally, it can be observed that CMOD scatter is lower at a higher displacement rate.
- At first glance, J_c values of specimens precracked with high ΔK did not seem to differ from low ΔK precracked specimens. However, somewhat higher J_c values are observed for high ΔK specimens. Based on this, the effect of the introduced fatigue crack can be seen, since higher J_c values indicated that the slightly higher plastic strain in front of the crack tip ‘delayed’ the cleavage fracture in the transition temperature region.

The effect of specimen thickness represents a specific challenge and leaves room for future analyses that will represent a continuation of this study. A lot has already been achieved in this field regarding the material in question, however, the studies shown here have certain limitations, which once again offer more possibilities for further analysis. Of particular interest is the scatter of J_c and r_c for specimens tested at -90 °C. Small values of r_c in specimens precracked with high ΔK can be attributed to the influence of a larger plastic strain zone around the crack tip, which counters the crack growth and reaches a small length at the moment of failure, whereas for specimens precracked with low ΔK it is the other way around. Another question resulting from these tests is the simultaneous application of displacement rate and specimen thickness analysis on the obtained results. Along with everything previously said on solving this problem, numerical methods are proposed as a means of obtaining good preliminary results, in accordance with expectations. Anyhow, the following needs to be taken into account: the scatter of results in transition temperature region makes result interpretations much harder. Hence, there is a need to increase the number of tests, but the challenge of adequate interpretation still remains.

ACKNOWLEDGEMENT

This work is supported by the Ministry of Education, Science and Technological Development of the Republic of Serbia (Contract No. 451-03-68/2020-14/200135).

REFERENCES

1. Garrison Jr., W.M., Moody, N.R. (1987), *Ductile fracture*, J Phys. Chem. Solids, 48(11): 1035-1074. doi: 10.1016/0022-3697(87)90118-1
2. Sedmak, S., Grabulov, V., Momčilović, D. (2009), *Chronology of lost structural integrity initiated from manufacturing defects in welded structures*, Struct. Integ. and Life, 9(1): 39-50.
3. Čamagić, I., et al. (2016), *Influence of temperature and exploitation period on the behaviour of a welded joint subjected to impact loading*, Struct. Integrity and Life, 16(3): 179-185.
4. Stewart, M., Lewis, O.T., Pressure Vessels Field Manual: 3. Materials Selection for Pressure Vessels, Common Operating Problems and Practical Solutions. 2013: 95-132. doi: 10.1016/B978-0-12-397015-2.00003-2
5. Kawiak, M., Kochmański, P. (2020), *Brittle fracture of the fifty-year-old pipeline support bearing*, Eng. Fail. Anal. 116. doi: 10.1016/j.engfailanal.2020.104770
6. Sedmak, A., Primena mehanike loma na integritet konstrukcija (monografija), (*Fracture Mechanics Applications in Structural Inegrity – monograph, in Serbian*), University of Belgrade, Faculty of Mechanical Eng., Belgrade, 2003.
7. Knott, J.F., Fundamentals of Fracture Mechanics, Butterworth & Co., 1973.
8. Hu, X., Duan, K. (2008), *Size effect and quasi-brittle fracture: the role of FPZ*, Int. J Fract. 154: 3-14. doi: 10.1007/s10704-008-9290-7
9. Argon, A.S. (2001), *Mechanics and physics of brittle to ductile transitions in fracture*, J Eng. Mater. Technol. 123(1): 1-11. doi: 10.1115/1.1325408
10. Čamagić, I., et al. (2017), *Impact of temperature and exploitation time on plane strain fracture toughness, K_{Ic}, in a welded joint*, Struct. Integ. and Life, 17(3): 239-244.
11. Berejnoi, C., Perez Ipiña, J.E. (2016), *Fracture Toughness of Ferritic Steels in the Ductile-to-Brittle Transition Region*, in Fracture Mechanics - Properties, Patterns and Behaviours – Ch.4, Intech, Ed. L.M. Alves, 2016. doi: 10.5772/63410
12. Anderson, T.L., Fracture Mechanics, Fundamentals and Application, 3rd Ed.., Taylor & Francis Group, 2005.
13. Lucon, E., McCowan, C.N., Santoyo, R.L., Impact Characterization of Line Pipe Steels by Means of Standard, Sub-Size and Miniaturized Charpy Specimens, NIST TN 1865, 2015. doi: 10.6028/NIST.TN.1865
14. Radović, N., Grabulov, V., Smiljanić, M., Antić, M. (2003), *Ni alloyed steels for low temperature service*, Zavarivanje i zavarene konstrukcije (*Welding and Welded Structures*), 48(1): 14-20.
15. Nankali, H.R. (2012), *Brittle-ductile transition zone case study (Zagros-Iran)*, J Asian Earth Sci. 59: 156-166. doi: 10.1016/j.jseaes.2012.07.011
16. Heerens, J., Reed, D.T. (1988), *Fracture behaviour of a pressure vessel steel in the ductile-to-brittle transition region*, in NISTIR 88-3099, GKSS Research Center, 1988, p.52.
17. Landes, J.D., Heerens, J., Schwalbe, K.-H., Petrovski, B. (1993), *Size, thickness and geometry effects on transition fracture*, Fatigue Fract. Engng. Mater. Struct. 16(11): 1135-1146. doi: 10.1111/j.1460-2695.1993.tb00729.x
18. Milne, I., Chell, G., *Effect of Size on the J Fracture Criterion*, in Elastic-Plastic Fracture (Eds. J. Landes, J. Begley, G. Clarke), STP668, 1979, West Conshohocken, PA, ASTM International. pp.358-377. doi: 10.1520/STP35839S
19. Wallin, K. (1985), *The size effect in K_{IC} results*, Eng. Fracture Mech. 22(1): 149-163. doi: 10.1016/0013-7944(85)90167-5
20. ASTM E399-12 Standard Test Method for Linear-Elastic Plane-Strain Fracture Toughness K_{Ic} of Metallic Materials, 2012. doi: 10.1520/E0399-12
21. ASTM E1820-16 Standard Test Method for Measurement of Fracture Toughness, 2016. doi: 10.1520/E1820-16
22. Sedmak, S., Burzić, Z., *Fracture mechanics standard testing*, in ‘Fracture Mechanics to Structural Integrity Assesment’, IFMASS 8, Monograph- Summer School of Fracture Mechanics, ISBN 86-905595-0-7, 2004, pp.95-122.
23. Kussmaul, K., Maile, K., Obst, V. (1987), *Influence of long-term thermal ageing on creep-fatigue behaviour of ferritic*

steels, Theor. Appl. Fract. Mech. 8(1): 1-9. doi: 10.1016/0167-8442(87)90012-7
24. Chowdhury, T., et al. (2015), *Incremental cyclic fracture behaviour of 20MnMoNi55 steel at room temperature*, Int. J Fract. 192(1): 117-132. doi: 10.1007/s10704-015-9990-8
25. ASTM E647-08 Standard Test Method for Measurement of Fatigue Crack Growth Rates, 2008. doi: 10.1520/E0647-08
26. Paris, P., Sih, G., *Stress Analysis of Cracks*, in Fracture Toughness Testing and its Applications, STP381, West Conshohocken, PA, ASTM Int., 1965, pp.30-81. doi: 10.1520/STP26584S
27. Čamagić, I., et al. (2013), *Compatibility of fracture mechanics parameters and fatigue crack growth parameters in welded joint behaviour evaluation*, Technical Gazzete, 20(2): 205-211.
28. Sedmak, S.A., et al. (2019), *Influence of welded joint microstructures on fatigue behaviour of specimens with a notch in the heat affected zone*, Eng. Fail. Anal. 106, 104162. doi: 10.1016/j.engfailanal.2019.104162
29. ASTM E1823-13 Standard Terminology Relating to Fatigue and Fracture Testing, 2013. doi: 10.1520/E1823-13

Fatigue 2021

March 29–31, 2021, Downing College, Cambridge, UK

This conference has been rescheduled from June 2020 and the majority of presentations will be delivered at the new event.

The conference is convened by the Engineering Integrity Society and is 8th in the series. More about the EIS at www.e-i-s.org.uk

Fatigue 2021 will bring the international fatigue and durability community together to share knowledge and understand challenges in using sophisticated engineering simulation and modelling tools to complement sound test programmes and develop reliable and cost effective products for modern usage.

As engineering modelling and simulation tools become ever more powerful and sophisticated there still remains the challenge of correlating the virtual world with both idealised laboratory testing and the wide, and potentially unexpected, range of service conditions experienced by machines and structures. These challenges are compounded by the advent of new materials, new ways of manufacturing components, new applications and new test and measurement techniques.

We shall seek to explore not only the latest developments in engineering modelling and simulation, advances in test and measurement techniques, innovations in manufacturing, and developments in materials science, but also the complex interrelations between these topics that give rise to improvements in fatigue performance, durability and structural integrity.

Convenor
John Yates (UK)

Contact: http://e-i-s.org.uk/contact/

Keynote Lectures

- *Very-high-cycle fatigue of additive manufactured materials,*
Professor Youshi Hong, Chinese Academy of Sciences

- *Fatigue-crack propagation in high-entropy alloys at ambient to cryogenic temperatures,*
Professor Robert Ritchie, University of California

- *50 years of Fatigue Research: Progress and Perspectives,*
Professor Roderick Smith, Imperial College

- *Overview of fatigue design in aerospace electrification,*
Mukesh Patel, Safran

LCF9 - Ninth International Conference On Low Cycle Fatigue

June 22-24, 2021, Berlin, Germany

Organization
German Association for Materials Research and Testing e.V.
Phone: +49 30 8113066 | Fax: +49 30 8119359
lcf9@dvm-berlin.de www.lcf9.de www.dvm-berlin.de

Scope

The permanent and growing interest of the scientific community in low-cycle fatigue, including thermomechanical fatigue addresses a broad range of applications, e.g. energy technology, transportation, civil engineering, and several other topics. Many questions on fundamental deformation and damage mechanisms, influence of multiaxial stresses/strains, creep-fatigue and TMF/HCF interaction and crack initiation and growth are investigated with increasing experimental efforts. As a bridge between fundamental research and application in component and structural design, simulation approaches for cyclic plasticity, crack initiation and growth have made impressive and still continuing progress in the recent decades: FEM-based deformation and life assessment models at different scales, state-of-the art and under further successful development, especially for reliable design of components are undergoing complex thermomechanical loadings. Increase in 2D-3D full-field measurements by image-volume correlation associated to high-fidelity FEM simulations are a major challenge.

The objective of LCF9 is to provide a worldwide platform for scientific communication and discussion and as a point of origin for collaboration of scientists and engineers interested in fundamental aspects and practical application and novel challenges in the context of digitalization.

Topics
Isothermal LCF, thermomech. fatigue (TMF) and multiaxial LCF
Superimposed LCF/HCF & TMF/HCF loads and creep-fatigue interaction
In-situ fatigue testing
Microstructural aspects of cyclic plasticity, fatigue damage, crack initiation and growth
Influence of surface, environment and protective coatings
Advanced materials and case studies
Novel experimental methods and standardization
Deform. & damage modelling and simulation based life assessment
Fatigue Research 4.0: Future approaches in data acquisition, handling and processing

Timeline
30th March 2020, submission of abstracts
June 2020, acceptance of papers
1st November 2020, start of Early Bird registration
1st March 2021, end of Early Bird registration, deadline for submission of full papers and registration
1st June 2021, tentative programme online, submission of power point presentations, final programme

Executive chairs
Tilmann Beck, Technische Universität Kaiserslautern, Germany
Eric Charkaluk, Ecole Polytechnique, Palaiseau, France